2014 IEEE International Conference on Robotics & Automation (ICRA)
Hong Kong Convention and Exhibition Center
May 31 - June 7, 2014. Hong Kong, China

Detection, Localization and Picking Up of Coil Springs from a Pile

Keitaro Ono[1], Takuya Ogawa[1], Yusuke Maeda[1],
Shigeki Nakatani[2], Go Nagayasu[2], Ryo Shimizu[2] and Noritaka Ouchi[2]

***Abstract*— Picking of parts loaded in bulk is an industrial need. Thus bin-picking systems for various objects have ever been studied by various ways. However, it is difficult to recognize coil springs randomly placed in a pile by conventional machine vision techniques because of their shape characteristics. In this paper, we propose a method of recognition and pose estimation of coil springs. This method uses their highlights made by illumination for their recognition and pose estimation with stereo vision. We implemented this method as a bin-picking system with an industrial robot. Bin-picking of coil springs was successfully demonstrated on the system. Position errors were less than 2 mm. The average success rate for a coil spring in the part box was 94% when multiple retrials of picking were allowed. This rate could be improved by implementation of collision avoidance.**

I. Introduction

Part feeders are widely used to supply parts loaded in bulk to production processes. However, they have many problems such as vibration, noise, damage and stops due to part jamming. Moreover, part feeders specialize in specific parts and require specialized jigs. Thus, bin-picking of various parts loaded in bulk is industrial need.

Bin-picking systems for various objects have ever been studied by various ways. Rahardja and Kosaka [1] proposed a bin-picking algorithm for complex objects. They used simple object features such as circles to recognize objects and estimate their pose. They conducted pose-estimation experiments with randomly cluttered alternator covers and demonstrated that the method is sufficient to be extended for actual grasping. Kirkegaard and Moeslund [2] applied Harmonic Shape Contexts features, which are invariant to translation, scale, and 3D rotation, to object localization. They matched these features from 3D data and CAD models to estimate object pose. They succeeded in correct pose estimation in presence of occlusion. Oh et al. [3] proposed a bin-picking system using several kinds of structured light. In this system, they estimated the pose of an object with geometric primitive information such as planes, columns, spheres and cones. They confirmed that an industrial robot could pick up randomly piled bolts. Domae et al. [4] demonstrated bin-picking of 13 kinds of parts including a coil spring. In this method, a depth map was segmented based on edges and appropriate segments to grasp objects were determined automatically. Shroff et al. [5] proposed a bin-picking system of detection and pose estimation using specular highlights. They used a multi-flash camera (MFC) to extract specular features and succeeded in bin-picking of screws. Liu et al. [6] proposed a fast directional chamfer matching (FDCM) algorithm, which uses line-segment approximations of edges, a three-dimensional distance transform and directional integral images. They succeeded in bin-picking of several kinds of objects. Nieuwenhuisen et al. [7] proposed a framework to grasp objects composed of shape primitives like cylinders and spheres. They generated shape compositions from CAD models and performed sub-graph matching with the primitives in scenes to detect and localize objects of interest. They demonstrated picking up an object consisting of a cylinder and two spheres from a transport box.

Coil springs are fundamental mechanical parts, but they are not dealt with in most of previous studies. Coil springs have the following shape characteristics:

- They have a succession of identical shapes.
- They have a complicated outline.
- They are see-through due to the openings in their shape.
- They have few planar sections.

Thus, coil springs do not have positive features for typical model-based image processing and therefore conventional bin-picking methods are not applicable.

Now, the purpose of this study is developing a reliable bin-picking system for coil springs. Our proposed method uses highlights on coil springs to detect them. Then we localize them with stereo vision for bin-picking.

II. Recognition of Coil Springs

II-A *Extraction and discrimination of highlights*

We focus on highlights which are made on coil springs by illumination. Highlights are usually avoided in machine vision but they are useful for recognition of coil springs. We binarize the image captured by a CCD camera (Fig. 1(a)) and the highlights (Fig. 1(b)) can be extracted. We classify them into side highlights (Fig. 1(c)) and end-face highlights (Fig. 1(d)) based on their areas as described in Fig. 2. The insides of end-face highlights are daubed with white. Hereafter, we process binarized images except for image matching explained in Section III-C.

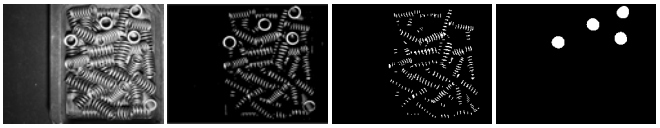

(a) source image (b) binary image (c) side highlights (d) end-face highlights

Fig. 1. Highlight Extraction

[1]Yokohama National University
[2]NHK SPRING CO., LTD.

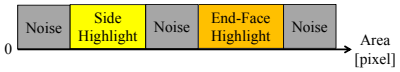

Fig. 2. Area-based Highlight Discrimination

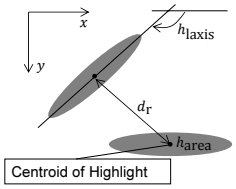

Fig. 3. Grouping Parameters h_{area}, h_{laxis}, d_{r}

(a) source image (b) grouping result

Fig. 4. An Example of Recognition

II-B Grouping of highlights

We group side highlights that belong to a coil spring into a highlight group using grouping parameters. The grouping parameters are the area of a highlight, h_{area}, the direction of the long axis of a highlight, h_{laxis}, the magnitude of the curve of a highlight, h_{cm} and the distance between highlights, d_{r} (Fig. 3). We define a $(p+q)$-dimensional image moment as m_{pq} and a $(p+q)$-dimensional center moment as μ_{pq} [8]. We also define a $(p+q)$-dimensional center moment in the rotated axes along h_{laxis} as μ'_{pq}. The grouping parameters are calculated as follows:

$$h_{\mathrm{area}} = m_{00}, \tag{1}$$

$$h_{\mathrm{laxis}} = \mathrm{atan2}\left(2\mu_{11}, \mu_{20} - \mu_{02}\right)/2, \tag{2}$$

$$h_{\mathrm{cm}} = \mu'_{21} / \left(\mu'_{20}\sqrt{\mu'_{02}}\right). \tag{3}$$

The distance between two highlights is the distance between their centroids.

The algorithm of grouping of highlights is described as follows:

1) Choose one highlight from all detected side highlights (a reference highlight).
   a) Choose one highlight from other side highlights (a chosen highlight).
   b) If grouping parameters of the reference highlight are similar to those of the chosen highlight, include the chosen highlight in the group of the reference highlight.
   c) Repeat a) and b) for all other side highlights.
2) Repeat 1) for all side highlights.

Side highlights of one spring must be in-line at even intervals. Thus after the above procedure, highlights whose centroids are not in-line or not at even intervals are excluded in every group.

Redundant highlight groups can be generated in the above procedure. Thus, we sort highlight groups according to the number of highlights included in each group. We adopt highlight groups in descending order and reject groups that include already adopted highlights.

End faces are nearly circular and therefore can be regarded as ellipses flattened according to their inclination in the camera image. Thus, we fit an ellipse to an end-face highlight to recognize and localize it.

II-C Recognition experiment

Fig. 4 is an example of recognition results of coil springs from an image from one camera. Recognized coil springs are colored separately in the figure. There are some coil springs which are not recognized because they are partly occluded by other coil springs. However, they are unsuited for picking at this time and can be recognized later as other coil springs are picked up and removed.

III. Stereo Correspondence

We estimate position and orientation of coil springs by stereo vision. In typical stereo vision methods, corresponding points from whole images of two cameras are detected and 3D information is obtained. However, there are problems of correspondence errors and calculation load. Those are prominent to coil springs because they do not have positive features for image processing as stated in Section I. Thus, we apply the recognition method described in Section II to each of the images of the two cameras and check correspondence only between recognized coil springs.

We set the two cameras so that their optical axes are parallel to each other and vertical to the reference horizontal plane for easy correspondence detection between left and right recognition results.

III-A Checking correspondence between highlight groups

We recognize coil springs in left and right images as highlight groups and check correspondence between them. The point to check correspondence is the centroids of highlights included in each of the groups. The algorithm of checking correspondence is explained as follows:

1) Rectify left and right images.
2) Recognize coil springs in each of the images as highlight groups.
3) Choose one group from the recognized groups in the left image (a left group).
   a) Check the following conditions for the left group and all groups recognized in the right image:
      Condition 1-1 The average areas of included highlights are nearly equal.
      Condition 1-2 The distance between the centroids of the groups g_{dis} is smaller than a threshold.
      Condition 1-3 The directions of the groups are nearly equal.
   b) Choose one right group for which condition 1-1, 1-2 and 1-3 are satisfied and g_{dis} is the smallest (a chosen right group).

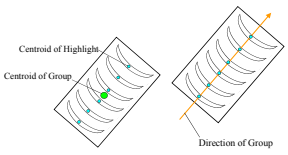

(a) centroid of group (b) direction of group

Fig. 5. Parameters of Group

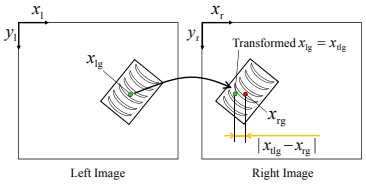

Fig. 6. Distance between Centroids of Left and Right Groups

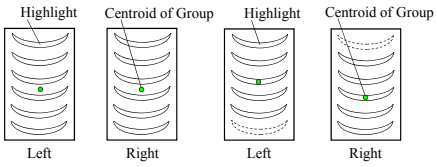

(a) one-to-one (b) not one-to-one

Fig. 7. Recognized Highlights for a Spring

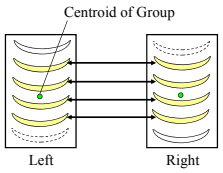

Fig. 8. Highlight Correspondence

c) If there is a chosen right group,
   i) Check the following conditions for the left group and the chosen right group:
      Condition 2-1 Numbers of highlights are nearly equal.
      Condition 2-2 Two y coordinates of the centroids of the groups are nearly equal.
   ii) If condition 2-1 and 2-2 are satisfied, the left group corresponds to the chosen right group.
   iii) If condition 2-1 or 2-2 are not satisfied, check correspondence of each highlight in the highlight groups as described in Section III-B.
d) If there is not the chosen right group, there is no correspondence.

4) Repeat 3) for all groups recognized in the left image.

The centroid of a highlight group is the average of centroids of highlights in the group (Fig. 5(a)). The direction of the group is that of the approximation line of centroids of highlights in the group (Fig. 5(b)). The distance between the centroids of the groups is defined by the following equation:

$$g_{\mathrm{dis}} = |x_{\mathrm{tlg}} - x_{\mathrm{rg}}|, \tag{4}$$

where x_{rg} is x coordinate of the centroid of the group in the right image (Fig. 6); x_{tlg} is defined by the following equation:

$$x_{\mathrm{tlg}} = x_{\mathrm{lg}} - fT/(L_{\mathrm{m}}P_s), \tag{5}$$

where x_{lg} is x coordinate of the centroid of the group in the left image, f is the focal length, T is the baseline length, L_{m} is the median of the possible depth of springs from the cameras and P_s is the pixel size of the cameras.

In regard to end-face highlights, we find correspondence of them if the area of the highlight and y coordinate of the center of the fitted ellipse in the left image are nearly equal to those in the right image, and the distance between the centers of the fitted ellipses is small. The corresponding points are the centers of the fitted ellipses.

III-B Checking correspondence between highlights in groups

We can find correspondence between highlight groups only if recognized highlights in the left and right images have one-to-one correspondence like Fig. 7(a) using the algorithm explained in Section III-A. If not one-to-one like Fig. 7(b), we cannot find group correspondence because the condition 2-1 or 2-2 are not satisfied. Thus, if the condition 2-1 or 2-2 are not satisfied, we check correspondence for each highlight in highlight groups like Fig. 8. Now the corresponding point of the highlight group is not the centroid of the group, but that of corresponding highlights in the group only. The algorithm of checking correspondence is as follows:

1) Choose one highlight from the left highlight group (a left highlight).
   a) Check the following conditions between the left highlight and highlights of the chosen right group:
      Condition 3-1 The distance between the centroids of the possibly corresponded highlights is smaller than a threshold.
      Condition 3-2 Two y coordinates of the centroids of the highlights are nearly equal.
   b) The left and right highlights for which condition 3-1 and 3-2 are satisfied and the distance between their centroids is the smallest correspond.
2) Repeat 1) for all highlights included in the left group.
3) Include only corresponding highlights in the groups.

III-C Checking correspondence between highlights in groups by image matching

If the direction of the group is nearly horizontal in camera images, we cannot find correct correspondence as shown in Fig. 9 using only binary highlight information, on which the algorithms explained in Section III-A and III-B depend. Thus, we check correspondence between highlights by image matching with not binary but source images in this case. The algorithm of checking correspondence between highlights by image matching is as follows (Fig. 10):

1) Consider a neighbor region of the left group in the left image as a template.
2) Consider a broader neighbor region of the right group in the right image as a search area.
3) Find a matched area in the search area by image matching with the template.
4) Choose one highlight from the left group (a left highlight).
   a) Define x coordinate of the centroid of the left highlight as d_{l}.
   b) Choose one highlight from the right group (a right highlight).
      i) Define x coordinate of the centroid of the right highlight as d_{r}.
      ii) If $|d_{\mathrm{l}} - d_{\mathrm{r}}|$ is smaller than a threshold, the left and right highlights correspond.

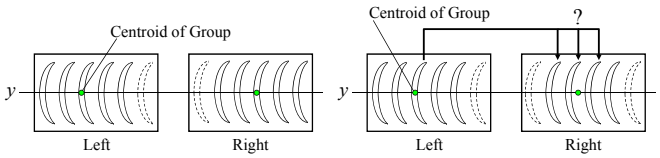

(a) same number of recognized highlights (b) different number of recognized highlights

Fig. 9. Possible Correspondence Confusion

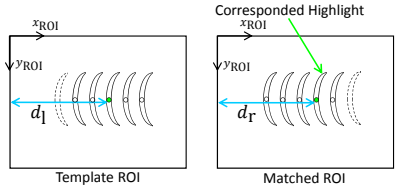

Fig. 10. Highlight Correspondence by Image Matching

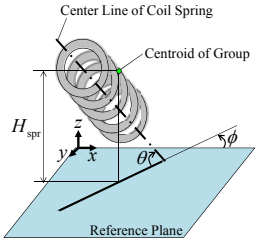

Fig. 11. Definition of Position and Orientation

c) Repeat b) for all highlights included in the right group.

5) Repeat 4) for all highlights included in the left group.
6) Include only corresponded highlights in the groups.

IV. Estimation of Position and Orientation

We can estimate position and orientation of coil springs from the stereo correspondence detected in Section III. We define the height of a coil spring, $H_{\rm spr}$ and its orientation, (θ, ϕ) as follows (Fig. 11):

- $H_{\rm spr}$: the distance between the centroid of the group and the reference horizontal plane.
- θ $(0 \leq \theta \leq 90^\circ)$: the angle between the center line of the coil spring and its projection to the reference plane.
- ϕ $(-90^\circ \leq \phi \leq 90^\circ)$: the angle between the projection to the reference plane and x-axis.

IV-A Estimation of vertical position

The depth of a coil spring L is calculated by the following equation using the focal length f, the baseline length T, the parallax $d_{\rm p}$ and the pixel size P_s from the theoretical formula of conventional stereo vision:

$$L = fT/(d_{\rm p}P_s). \tag{6}$$

We define the distance between each of the cameras and the reference plane as L_0. The height of the coil spring is calculated by the following equation:

$$H_{\rm spr} = L_0 - L = L_0 - fT/(d_{\rm p}P_s). \tag{7}$$

Equation (7) has an error because the shapes of left and right highlights are not strictly identical due to the positional relationship among them and the light source and due to the curvature of coil springs. Thus, we modify the parallax of side highlights for error correction by the following equation:

$$d_{\rm p} \rightarrow d_{\rm p} + (a\phi + bd_{\rm p} + c), \tag{8}$$

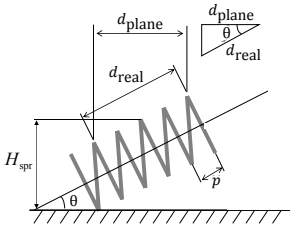

Fig. 12. Estimation of Orientation

Fig. 13. Image of the Coil Spring

TABLE I
Parameters of Cameras

$w \times h$	1296×964
P_s	3.45 [μm/pixel]
f	16 [mm]
T	51 [mm]
L_0	782 [mm]

TABLE II
Specifications of Coil Spring

external diameter	18 [mm]
free length	34 [mm]
end shape	closed end
end processing	polished
pitch	5 [mm]

where a, b and c are empirical coefficients estimated by experiments.

IV-B Estimation of horizontal position

We define the CCD size as (W', V') and resolution as $w \times h$. The theoretical formula of horizontal position $A_{\rm L}$ is the following equation:

$$A_{\rm L} = \left(\frac{L}{f}\frac{W'}{w}\left(x_{\rm p} - \frac{w}{2}\right), \frac{L}{f}\frac{V'}{h}\left(y_{\rm p} - \frac{h}{2}\right)\right), \tag{9}$$

where $(x_{\rm p}, y_{\rm p})$ is the point on the image.

IV-C Estimation of orientation

The inclination of the coil spring θ is calculated by the following equation from Fig. 12:

$$\theta = \cos^{-1}\left(d_{\rm plane}/d_{\rm real}\right), \tag{10}$$

where $d_{\rm plane}$ is the actual length of the highlight group, $d_{\rm real}$ is the length of the coil spring. $d_{\rm plane}$ is calculated by the following equation:

$$d_{\rm plane} = LP_sD_{\rm plane}/f, \tag{11}$$

where $D_{\rm plane}$ is the length of the highlight group on the image.

V. Experiments of Correspondence Detection and Pose Estimation

V-A Experimental environment

We use two grayscale CCD cameras, Point Grey Research FL2G-13S2M. Table I shows parameters of them. We use an LED spotlight to make highlights of coil springs. All the computation was performed on a PC with Intel Core i7 860 CPU on Ubuntu 9.04 64bit OS. Coefficients for error correction of parallax are as follows: $a = 1.63 \times 10^{-2}$ [pixel/deg], $b = -1.67 \times 10^{-2}$ [$-$], $c = 5.0$ [pixel]. We call this experimental setup Environment A. Fig. 13 shows a coil spring used in this experiment. Table II shows the specification of the coil spring.

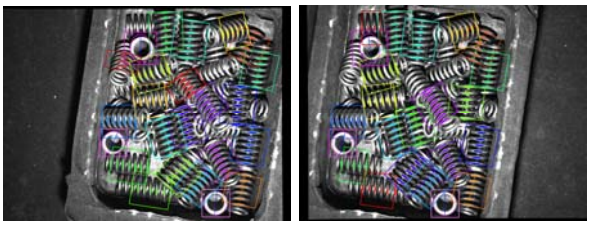

(a) grouping result (left) (b) grouping result (right)

(c) correspondence result w/o image matching (left) (d) correspondence result w/o image matching (right)

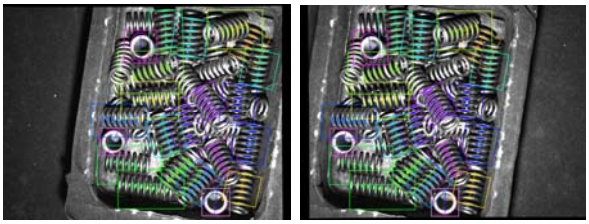

(e) correspondence result w/ image matching (left) (f) correspondence result w/ image matching (right)

Fig. 14. An Example of Recognition Results

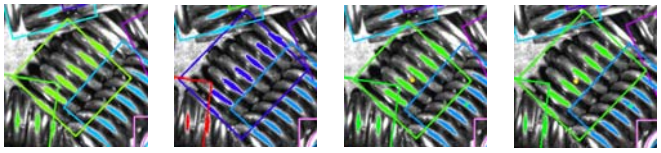

(a) grouping result (left) (b) grouping result (right) (c) found correspondence (left and right)

Fig. 15. Correspondence between Non-horizontal Highlight Groups

V-B *Experiments of correspondence detection*

Fig. 14 is an example of results of correspondence detection. Left images of Fig. 14 are identical to Fig. 4. Corresponded springs in the left image and the right image are shown in the same color. Fig. 15 is a magnification of a specific coil spring in Fig. 14. Although the recognized highlights in the left image did not have one-to-one correspondence with those in the right image, correspondence was found correctly. Fig. 16 is also a magnification of a specific coil spring in Fig. 14. When the image matching algorithm was applied, correspondence between highlights in groups whose directions were nearly horizontal in the camera images was found correctly.

V-C *Experiments of pose estimation*

We placed a single spring like Fig. 17 and estimated its position and orientation. Table III shows the average absolute error between the true and estimated values.

When $\theta = 0$ [deg], the error of orientation is about 15 [deg] mainly due to the sensibility of $\cos^{-1}$. Although it seems large, it is acceptable for bin-picking.

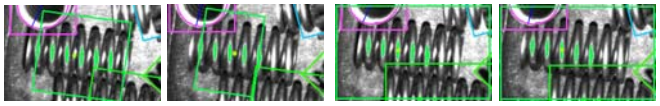

(a) incorrect correspondence w/o image matching (left and right) (b) found correspondence w/ image matching (left and right)

Fig. 16. Correspondence between Horizontal Highlight Groups

(a) $\theta = 90°$ (b) $\theta = 0$ (c) $0 < \theta < 90°$

Fig. 17. Source Images of Left Camera

VI. Construction of a Bin-picking System

VI-A *Picking strategy*

In our bin-picking system, outer side of the coil spring is grasped by two fingers of a gripper. The gripper is horizontally positioned at the centroid of the highlight group if $\theta = 0$ (Fig. 18(a)), at the higher end of the group if $0 < \theta < 90°$ (Fig. 18(b)), and at the center of the ellipse of the end-face highlight if $\theta = 90°$ (Fig. 18(c)), respectively.

Basically the highest coil spring is picked up first. However, when its picking fails, we skip it and try the second highest one.

VI-B *Experimental setup*

Fig. 19 shows our experimental setup. We used a manipulator, Mitsubishi Electric Corporation RV-1A with an electric gripper, in addition to the two CCD cameras and the spot light used in Environment A.

TABLE III
Estimation Results

	Average Error	
	ΔH_{spr} [mm]	$\Delta\theta$ [deg]
$\theta = 90°$	1.3	—
$\theta = 0$	0.7	15
$0 < \theta < 90°$	0.8	2

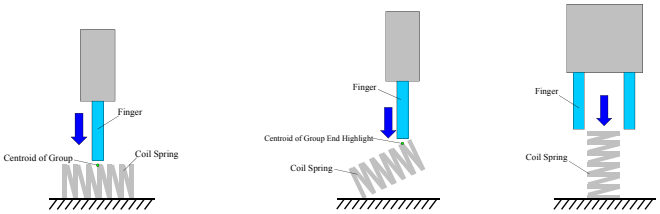

(a) $\theta = 0$ (b) $0 < \theta < 90°$ (c) $\theta = 90°$

Fig. 18. Grasping Approach

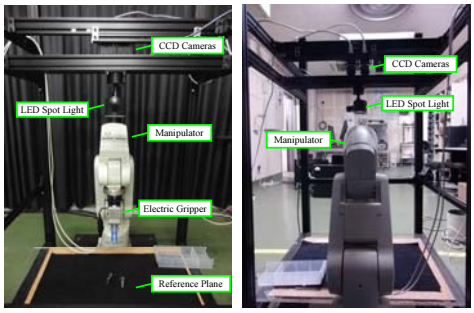

(a) front view (b) back view

Fig. 19. Experimental Environment

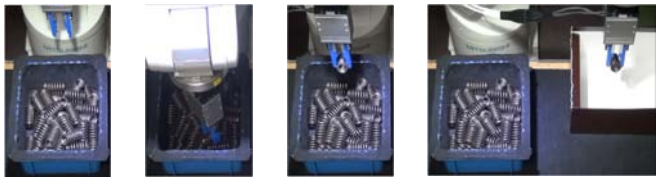

Fig. 20. Bin-picking

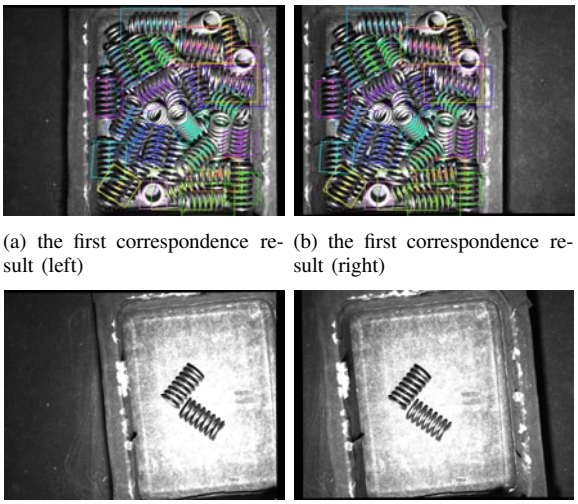

(a) the first correspondence result (left) (b) the first correspondence result (right)

(c) the last correspondence result (left) (d) the last correspondence result (right)

Fig. 21. An Example of Correspondence Results

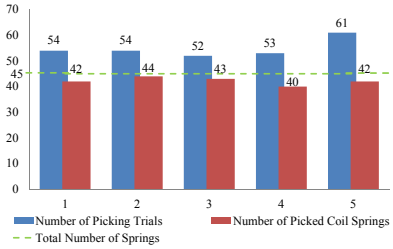

Fig. 22. Picking Results in Five Experiments

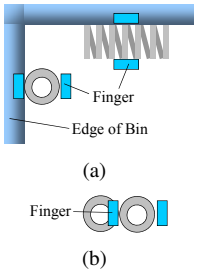

Fig. 23. Possible Collisions

VI-C Experimental results

First, one coil spring was placed as shown in Fig. 17. The isolated coil spring was successfully picked up in all the placements. The accuracy of the estimation of its horizontal position was under 1 [mm].

Next, forty-five coil springs were loaded in a part box and picked up. Five experiments of bin-picking were conducted. Fig. 20 shows some scenes of bin-picking. Fig. 21 shows the first and the last correspondence result of a bin-picking experiment. At last, two coil springs could not be recognized because of halation of the bottom of the bin. The accompanying video shows another bin-picking experiment. The time for recognition of coil springs and pose estimation was about 1.7 [s]. Fig. 22 shows the number of picking trials and the number of picked coil springs in each experiment. The average success rate for each picking trial was 77% in five experiments, and the average success rate for a coil spring in the part box was 94% when multiple retrials of picking were allowed. The main reason for the failure in picking was collisions between the fingers of the gripper and the part box, and those between the fingers and other coil springs. When coil springs are in the edge of the part box or upright coil springs are lined up like Fig. 23, bin-picking may fail due to our naive implementation in which collisions are not considered. In order to solve this problem, we need to check collisions before picking and choose collision-free grasping paths.

VII. Conclusions

In this study, we developed a method to recognize coil springs with their highlights and estimate their position and orientation by stereo vision. Horizontal and vertical accuracy of estimation was under 1 [mm] and under 2 [mm], respectively. Calculation time was about 1.7 [s], which is short enough to complete during pick-and-place of a previous coil spring. We also developed a bin-picking system using this method. The average success rate of each picking trial for randomly placed coil springs was 77%, and that of a coil spring when multiple retrials were allowed was 94%. The main reason for picking failure was collisions between the gripper and obstacles, and therefore collision avoidance would improve the reliability of bin-picking significantly.

References

[1] K. Rahardja and A. Kosaka: "Vision-based Bin-Picking: Recognition and Localization of Multiple Complex Objects using Simple Visual Cues," Proc. of 1996 IEEE/RSJ Int. Conf. on Intelligent Robots and Systems, vol. 3, pp. 1448–1457, 1996.

[2] J. Kirkegaard and T. B. Moeslund: "Bin-Picking based on Harmonic Shape Contexts and Graph-Based Matching," Proc. of 18th Int. Conf. on Pattern Recognition, vol. 2, pp. 581–584, 2006.

[3] J.-K. Oh et al.: "Development of Structured Light based Bin Picking System Using Primitive Models," Proc. of 2009 IEEE Int. Symp. on Assembly and Manufacturing, pp. 46–51, 2009.

[4] Y. Domae et al.: Proc. of the 29th Annu. Conf. of Robotics Soc. of Japan, RSJ2011AC3B2-1, 2011. (in Japanese)

[5] N. Shroff et al.: "Finding Needle In A Specular Haystack," Proc. 2011 IEEE Int. Conf. on Robotics and Automation, pp. 5963–5970, 2011.

[6] M.-Y. Liu et al.: "Fast object localization and pose estimation in heavy clutter for robotic bin picking," Int. J. of Robotics Research, vol. 31, no. 8, pp. 951–973, 2012.

[7] M. Nieuwenhuisen et al.: "Shape-Primitive Based Object Recognition and Grasping," Proc. of 7th German Conf. on Robotics, 2012.

[8] R. Mukundan and K. R. Ramakrishnan: "Moment functions in image analysis: theory and applications," World Scientific, 1998.